 CMES, vol.2, no.2, pp.195-212, 2001

On Finite Element Analysis of Fluid Flows Fully Coupled with Structural Interactions

S. Rugonyi, K. J. Bathe[1]

Abstract: The solution of fluid flows, modeled using the Navier-Stokes or Euler equations, fully coupled with structures/solids is considered. Simultaneous and partitioned solution procedures, used in the solution of the coupled equations, are briefly discussed, and advantages and disadvantages of their use are mentioned. In addition, a simplified stability analysis of the interface equations is presented, and unconditional stability for certain choices of time integration schemes is shown. Furthermore, the long-term dynamic stability of fluid-structure interaction systems is assessed by the use of Lyapunov characteristic exponents, which allow differentiating between a chaotic and a regular system behavior. Some state-of-the-art numerical solutions are also presented to indicate the type of problems that can now be solved using currently available techniques.

keyword: Fluid-structure interaction, arbitrary Lagrangian-Eulerian formulation, finite element methods, coupled procedures, Lyapunov characteristic exponent, dynamic stability.

1 Introduction

The analysis of a coupled multi-physics system is frequently required today to understand (and optimize) the behavior of the system. In particular, the analysis of problems that involve fluid flows interacting with solids or structures is increasingly needed in diverse applications including biomechanical systems, micromechanical devices, the optimization and control of brake systems, pumps, or computer disk readers; to mention just a few. As a consequence, the development of more effective finite element methods for the solution of fluid-structure interaction (FSI) problems is important.

Different strategies have been proposed to solve FSI problems, and the selection of the most effective approach strongly depends on the characteristics of the problem to be analyzed. Specifically, the mathematical model employed in the description of the fluid behavior plays a decisive role in the selection of the most suited solution procedure. For example, if the fluid is modeled using the acoustic approximation, a potential formulation can be used to solve the problem and the degrees of freedom of the fluid are reduced to one per node. The fluid equations can then be coupled to the structural equations in an effective manner by using the ϕ-formulation [Olson and Bathe (1985)] [Bathe (1996)], which results in a symmetric coefficient matrix for the coupled problem. Other simultaneous solution procedures for the acoustic fluid model have also been proposed in [Wang and Bathe (1997)]. Alternatively, the coupled FSI equations can be solved using partitioned procedures, see [Park, Felippa and DeRuntz (1977)]. Additional FSI models are discussed in [Morand and Ohayon (1995)].

If the fluid is modeled using the Navier-Stokes or Euler equations, two cases can be distinguished. The first case occurs when there is a weak interaction between the fluid and the structure; then the structure and fluid domains barely deform. The second case occurs when the interaction results in a strong coupling between the fluid flow and the structure, and the fluid and solid domains might then undergo large deformations.

The main approaches employed in the solution of FSI problems are the simultaneous (direct) and the partitioned (iterative) solution procedures. In the simultaneous solution procedure the fluid and solid equations are established and solved together. In a partitioned procedure, each field (fluid and solid) is solved separately and solution variables (forces, or velocities and displacements at the interface) are passed iteratively from one field to the other until convergence is achieved (for each time or load step). It should be pointed out that a full coupling between the media is achieved by using any of the above-mentioned procedures. Usually, partitioned procedures are preferred when the interaction between the fluid

[1] MIT, Cambridge, MA, USA.

and the structure is weak and the simultaneous solution procedure is employed when there is a strong coupling.

In the next section, the equations that govern the behavior of fluids modeled using the Navier-Stokes equations and general structures are considered, together with the conditions that must be satisfied at the fluid-structure interfaces. The finite element discretization of the equations is considered in Section 3. Subsequently, in Section 4, the partitioned and simultaneous solution procedures are briefly discussed in the context of FSI problems. In addition, a simplified numerical stability analysis for the coupled equations at the interface is presented. In Section 5, the long-term stability of systems is addressed and the calculation of Lyapunov characteristic exponents of FSI systems discretized using finite element methods is presented. In Section 6 some examples of application that demonstrate the current capability of finite element methods in the solution of fluid-structure interaction problems are presented and finally in Section 7 the conclusions are given.

2 Problem Formulation

To model the behavior of solid media the Lagrangian formulation of motion is employed (i.e. particles are followed in their movement), whereas, for a fluid flow analysis the Eulerian formulation is usually used since it is of interest to know the behavior of the fluid at a particular position in space. However, when considering a fluid flow interacting with a solid medium and/or a fluid with a free surface, the fluid domain changes as a function of time, and an arbitrary Lagrangian-Eulerian (ALE) description of motion is needed. The ALE formulation is a combination of the Eulerian and Lagrangian descriptions, and has been discussed, for instance, in [Donea (1983)].

We will concentrate in this paper on the analysis of fluid flows interacting with structures that can deform and undergo large displacements. The fluid flow equations are modeled using the Navier-Stokes or Euler equations of motion, and the constitutive relations of the structure are assumed to be either linear or nonlinear.

2.1 Structural Equations

The Lagrangian equations of motion of the structure are

$$\rho \frac{\partial^2 \mathbf{u}}{\partial t^2} = \nabla \cdot \tau + \mathbf{f}^B \tag{1}$$

where ρ is the density, $\mathbf{u}$ is the vector of structural displacements, t is the time, τ is the Cauchy stress tensor, $\mathbf{f}^B$ is the vector of body forces, and $(\nabla\cdot)$ represents the divergence operator (in the deformed configuration). Equations (1) can be linear or nonlinear, depending on the constitutive relations used for the material in consideration and whether the displacements are small or large [Bathe(1996)][Atluri(1984)].

The boundary conditions needed to solve Eq. (1) are,

$$\begin{aligned} \mathbf{u} &= \mathbf{u}_S \quad on \quad S_u \\ \tau \cdot \mathbf{n} &= \mathbf{f}^S \quad on \quad S_f \end{aligned} \tag{2}$$

where S_u and S_f represent the parts of the boundary with prescribed displacements, $\mathbf{u}_s$, and tractions, $\mathbf{f}^S$, respectively; and $\mathbf{n}$ is a unit outward normal vector to the boundary.

2.2 Fluid Flow Equations

The equations of motion of a compressible Newtonian fluid flow in the ALE description of motion are

$$\rho \frac{\delta \mathbf{v}}{\delta t} + \rho \left[(\mathbf{v} - \hat{\mathbf{v}}) \cdot \nabla \right] \mathbf{v} = \nabla \cdot \tau + \mathbf{f}^B \tag{3}$$

$$\frac{\delta \rho}{\delta t} + (\mathbf{v} - \hat{\mathbf{v}}) \cdot \nabla \rho + \rho \nabla \cdot \mathbf{v} = 0 \tag{4}$$

$$\rho \frac{\delta e}{\delta t} + \rho \, (\mathbf{v} - \hat{\mathbf{v}}) \cdot \nabla e = \tau \cdot \mathbf{D} - \nabla \cdot \mathbf{q} + q^B \tag{5}$$

where ρ here is the fluid density; $\delta/\delta t$ is the total time derivative "seen" by a probe moving with the ALE frame; $\mathbf{v}$ is the fluid velocity; $\hat{\mathbf{v}}$ is the velocity of the moving ALE frame; τ is the fluid stress tensor; $\mathbf{f}^B$ represents the vector of fluid body forces; e is the specific internal energy; $\mathbf{D}$ is the velocity strain (rate-of-strain) tensor, $2\mathbf{D} = \nabla\mathbf{v} + (\nabla\mathbf{v})^T$; $\mathbf{q}$ is the heat flux vector; q^B is the rate of heat generated per unit volume; $(\nabla\cdot)$ and (∇) represent the divergence and gradient operators respectively and $(\cdot)$ indicates internal product. Equation (3) is the momentum equation and (4) and (5) are the equations of conservation of mass and energy respectively. Note that in Eqs. (3) to (5), if $\hat{\mathbf{v}} = \mathbf{0}$, and therefore the ALE frame (or mesh in a finite element discretization) is not moving, the Eulerian formulation is recovered. Furthermore, if $\hat{\mathbf{v}} = \mathbf{v}$, that is, the ALE frame is moving with the fluid particles, the Lagrangian formulation of motion is recovered.

The constitutive relations for a Newtonian fluid are

$$\tau = \left[-p + \lambda \nabla \cdot \mathbf{v} \right] \mathbf{I} + 2\mu \mathbf{D} \tag{6}$$

where p is the fluid pressure, $\mathbf{I}$ is the identity tensor, μ and λ are the first and second coefficients of viscosity. For a wide variety of conditions the Stokes hypothesis

$$\lambda = -\frac{2}{3}\mu \tag{7}$$

accurately describes the behavior of the fluid flow and therefore it is generally used.

The constitutive equations for the heat transfer inside the body are

$$\mathbf{q} = -\mathbf{k}\nabla\theta \tag{8}$$

where $\mathbf{k}$ is the conductivity tensor (which reduces to a single value in the case of an isotropic medium), and θ is the temperature.

In addition, state equations are needed to solve Eqs. (3) to (5),

$$\rho = \rho(p,\theta) \tag{9}$$
$$e = e(p,\theta) \tag{10}$$

Note that in the case of an incompressible fluid, the density (of each fluid particle) is not a function of time and Eq. (4) reduces to $\nabla\cdot\mathbf{v} = 0$. Furthermore, Eqs. (3) and (4) are sufficient to solve for the isothermal behavior of an incompressible fluid flow, and hence the energy equation (5) need not be considered. However, Eqs. (3) to (5) need to be solved simultaneously when the solution of a compressible fluid is sought.

The Euler equations of motion are used when the fluid viscosity is neglected in the model.

The boundary conditions required to solve Eqs. (3) to (5) in the most general case of a compressible fluid are beyond the scope of this paper (since different situations such as supersonic/subsonic flow, viscous/non-viscous flow have to be considered). The interested reader is referred to [Bathe, Zhang and Zhang (1997)] in which a table with different boundary conditions is given.

Moving boundaries, free surfaces, as well as fluid-fluid interfaces can be considered when employing the ALE formulation for the fluid flow equations.

In the case of moving boundaries, the condition that must be satisfied is

$$\begin{aligned} \hat{\mathbf{u}}\cdot\mathbf{n} &= \hat{u}_s \quad \text{on} \quad S_{\hat{u}} \\ \hat{\mathbf{u}}\cdot\mathbf{t} &= \hat{u}_t \quad \text{on} \quad S_{\hat{u}} \end{aligned} \tag{11}$$

where $S_{\hat{u}}$ corresponds to the part of the surface with imposed displacements $\hat{u}_s$ and $\hat{u}_t$ in the normal and tangential directions respectively, $\mathbf{n}$ and $\mathbf{t}$ are unit normal and tangent vectors to the boundary, and $\hat{\mathbf{u}}$ is the boundary displacement. Note that the second of Eqs. (11) does not apply if the fluid is modeled as inviscid.

When a fluid-fluid interface is considered, compatibility and equilibrium conditions must be satisfied at the interface. The compatibility condition guarantees that the velocities of the particles at the interface are the same for both fluids considered (no slip condition) if both fluids are viscous, or that the normal component of the velocities to the interface are equal for both fluids (slip condition) if at least one of the fluids is assumed to be inviscid. The equilibrium condition at a fluid-fluid interface is

$$(\tau_2 - \tau_1)\cdot\mathbf{n} = \alpha\left(\frac{1}{R_1} + \frac{1}{R_2}\right)\mathbf{n} \tag{12}$$

where τ_1 and $\tau_2$are the stress tensors corresponding to the two interacting fluids, $\mathbf{n}$ is a unit normal vector to the interface surface pointing outward of surface 1, α is the coefficient of surface tension between the fluids, and R_1 and R_2 are the principal radii of curvatures of the interface surface (which are assumed to be positive if the center of curvature is on the side of the fluid 1 and negative otherwise). Note that if surface tension effects are neglected, $\alpha = 0$ in Eq. (12).

In case a free surface is considered, Eq. (12) is also applicable. However, the effect of one fluid (typically air) is usually included only as a pressure p_0(i.e. the fluid is assumed to be inviscid). Then, for a free surface, Eq. (12) is replaced by

$$-p_0\,\mathbf{n} - \tau\cdot\mathbf{n} = \alpha\left(\frac{1}{R_1} + \frac{1}{R_2}\right)\mathbf{n} \tag{13}$$

where $\mathbf{n}$ here points outward of the free surface, and the radii of curvature are assumed to be positive if their center is on the side of the modeled fluid.

Since only one fluid is now explicitly considered in the model, Eq. (13) is not sufficient to describe the motion of the free surface, and an additional equation is needed. Assume that the surface at a reference time t_0 is represented by the function $S({}^0\mathbf{x}, \mathbf{t}_0) = 0$, where ${}^0\mathbf{x}$ is the vector of coordinates of the particles that are located on the free surface at time t_0. The following condition must be satisfied,

$$\frac{\delta S}{\delta t} + (\mathbf{v} - \hat{\mathbf{v}})\cdot\nabla S = 0 \tag{14}$$

which ensures that the particles that are at the free surface at time t_0 will remain on that surface for all times.

2.3 Interface Between Fluid Flow and Solid

In a problem in which a viscous fluid flow is interacting with a solid medium, equilibrium and compatibility conditions must be satisfied at the fluid-structure interface. These conditions are

$$\tau^S \cdot \mathbf{n} = \tau^F \cdot \mathbf{n} \tag{15}$$

$$\begin{aligned} &\mathbf{u}^I(t) = \hat{\mathbf{u}}^I(t) \\ &\dot{\mathbf{u}}^I(t) = \mathbf{v}^I(t) = \hat{\mathbf{v}}^I(t) \\ &\ddot{\mathbf{u}}^I(t) = \dot{\mathbf{v}}^I(t) = \dot{\hat{\mathbf{v}}}^I(t) \end{aligned} \tag{16}$$

where $\mathbf{n}$ is a unit vector normal to the fluid-solid interface, $\mathbf{u}$ and $\hat{\mathbf{u}}$ are the displacements of the structure and the fluid domain (or mesh in a finite element analysis), respectively, $\mathbf{v}$ is the fluid velocity and $\hat{\mathbf{v}}$ the velocity of the fluid domain, the dot represents a time derivative, and the superscripts I, S and F denote the interface, and the solid and fluid media, respectivly.

3 Finite Element Discretization

Equations (1) and (3) to (5) can be discretized using the finite element procedure (see for example [Bathe (1996)]). Note that since the fluid flow equations are expressed using the ALE formulation of motion, the unknowns to be calculated include the displacements of the finite element mesh nodes.

In the following, for simplicity of exposition, the (almost) incompressible Navier-Stokes equations will be considered in the modeling of the fluid flow together with the equations of a general solid medium discretized using the displacement or displacement/pressure (u/p) formulations. In addition, thermal effects will not be included. The equations corresponding to the fluid and solid media will be coupled and different techniques to solve them briefly explained.

3.1 Structure/Solid Discretized Equations

The linearized discrete equations of a structure/solid medium (without dissipation) at time t can be expressed as follows

$$\mathbf{M}_u \ddot{\mathbf{u}} + \mathbf{K}_u \mathbf{u} = \mathbf{R}_u - \mathbf{F}_u \tag{17}$$

where $\mathbf{M}_u$ and $\mathbf{K}_u$ are the mass matrix and tangent stiffness matrix respectively, $\mathbf{u}$ here is the vector of *incremental* nodal point displacements, $\mathbf{R}_u$ is the vector of externally applied forces and $\mathbf{F}_u$ contains known terms of the linearization. If the structural response is linear, then the same equations are applicable except that $\mathbf{F}_u$ can be set equal to zero and, as a consequence, $\mathbf{u}$ corresponds to the vector of total nodal point displacements (not increments). If a u/p finite element formulation is employed to discretize the structural equations, then pressures must be included in $\mathbf{u}$ [Bathe(1996)].

3.2 Fluid Flow Discretized Equations

For the ALE fluid flow equations of motion, the linearized Navier-Stokes discrete equations can be represented by

$$\begin{bmatrix} \mathbf{M}_v & \hat{\mathbf{M}}_v \end{bmatrix} \begin{bmatrix} \dot{\mathbf{v}} \\ \dot{\hat{\mathbf{v}}} \end{bmatrix} + \begin{bmatrix} \mathbf{K}_v & \hat{\mathbf{K}}_v \end{bmatrix} \begin{bmatrix} \mathbf{v} \\ \hat{\mathbf{u}} \end{bmatrix} = \mathbf{R}_v - \mathbf{F}_v \tag{18}$$

where $\mathbf{M}_v$ and $\mathbf{K}_v$ are the mass and tangent coefficient matrices of the fluid flow, $\hat{\mathbf{M}}_v$ and $\hat{\mathbf{K}}_v$ are tangent mass and coefficient matrices corresponding to the linearized ALE terms which couple with the mesh movement, $\mathbf{v}$ is the vector of *incremental* nodal point velocities, $\hat{\mathbf{u}}$ and $\hat{\mathbf{v}}$ are the vectors of *incremental* mesh displacements and velocities, $\mathbf{R}_v$ is the vector of discretized externally applied forces and $\mathbf{F}_v$ contains known terms from the linearization. Pressure terms were omitted for simplicity.

The nodal point displacements of the mesh are calculated at FSI interfaces, free surfaces or fluid-fluid interfaces, and are prescribed at other moving boundaries. On the other hand, the displacements of internal mesh nodes (those that are not on an interface) can be arbitrarily specified with the objective to keep the mesh regular at all times. Different procedures are used in practice to calculate the mesh movement. One of the most popular ways of obtaining the movement of internal fluid nodes includes solving a Laplace or pseudo-structural equation for the mesh with boundary conditions given by the displacements of the mesh at interface surfaces or moving boundaries. This approach is usually efficient if the fluid mesh does not become too distorted. For problems in which the fluid domain changes drastically from the initial condition to some intermediate configuration, the mesh-updating procedure requires the use of more advanced techniques such as to allow the mesh nodes to

slip along interfaces, the use of leader-follower nodes and mesh repair procedures [Bathe, Zhang and Zhang (1997)].

3.2 Coupled Fluid Flow and Structural Equations

To solve an FSI problem using finite element methods, the discrete Eqs. (17) and (18) can be coupled using the equilibrium and kinematic conditions at the interface, Eqs. (15) and (16), as described in [Rugonyi and Bathe (2000)].

Using the superscripts I, F, and S to indicate fluid/structure interface and interior fluid and structure/solid degrees of freedom respectively, and assuming that no external forces are applied at the interface, the equilibrium condition (15) can be expressed as

$$\mathbf{R}_u^I + \mathbf{R}_v^I = \mathbf{0} \tag{19}$$

and the compatibility condition (16) is

$$\begin{aligned} \mathbf{u}^I &= \hat{\mathbf{u}}^I \\ \dot{\mathbf{u}}^I &= \hat{\mathbf{v}}^I = \mathbf{v}^I \\ \ddot{\mathbf{u}}^I &= \dot{\mathbf{v}}^I \end{aligned} \tag{20}$$

where here, following Eqs. (17) and (18), $\mathbf{u}$, $\hat{\mathbf{u}}$ and $\hat{\mathbf{v}}$ are the increments in the nodal displacements, mesh displacements and mesh velocities (and clearly the total nodal displacements, mesh displacements and mesh velocities satisfy the same equations).

The third of conditions (20) is usually difficult to satisfy and actually not satisfied exactly in general for all time. However, the condition can be relaxed provided the solution of the (linearized) coupled equations is obtained with a numerically unconditional stable time integration scheme. This issue is addressed below.

Since the movement of the interior mesh nodes is a function of the movement of the interface nodes (or in general the boundary nodes), it will be assumed, for simplicity of notation, that the effect of the mesh motion is contained in the matrices $\hat{\mathbf{M}}_\mathbf{v}$ and $\hat{\mathbf{K}}_v$ and that the mesh motion is applied to the interface degrees of freedom only. Separating the interface degrees of freedom from the degrees of freedom of the interior nodes, Eq. (18) is now expressed as,

$$\begin{bmatrix} \mathbf{M}_v^{II} & \mathbf{M}_v^{IF} \\ \mathbf{M}_v^{FI} & \mathbf{M}_v^{FF} \end{bmatrix} \begin{bmatrix} \dot{\mathbf{v}}^I \\ \dot{\mathbf{v}}^F \end{bmatrix} + \begin{bmatrix} \mathbf{K}_v^{II} + \hat{\mathbf{M}}_v^{II} & \mathbf{K}_v^{IF} \\ \mathbf{K}_v^{FI} + \hat{\mathbf{M}}_v^{FI} & \mathbf{K}_v^{FF} \end{bmatrix} \times \begin{bmatrix} \mathbf{v}^I \\ \mathbf{v}^F \end{bmatrix} + \begin{bmatrix} \hat{\mathbf{K}}_v^{II} & \mathbf{0} \\ \hat{\mathbf{K}}_v^{FI} & \mathbf{0} \end{bmatrix} \begin{bmatrix} \mathbf{u}^I \\ \mathbf{u}^F \end{bmatrix} = \begin{bmatrix} \mathbf{R}_v^I \\ \mathbf{R}_v^F \end{bmatrix} - \begin{bmatrix} \mathbf{F}_v^I \\ \mathbf{F}_v^F \end{bmatrix} \tag{21}$$

where $\mathbf{u}^F$ corresponds to the vector of increments of internal fluid particle displacements which are of course not calculated.

Using Eqs. (17), and (19) to (21), the coupled FSI equations are

$$\mathbf{A}\ddot{\mathbf{U}} + \mathbf{B}\dot{\mathbf{U}} + \mathbf{C}\mathbf{U} = \mathbf{G} \tag{22}$$

where

$$\mathbf{A} = \begin{bmatrix} \mathbf{M}_u^{SS} & \mathbf{M}_u^{SI} & \mathbf{0} \\ \mathbf{M}_u^{IS} & \mathbf{M}_u^{II} + \mathbf{M}_v^{II} & \mathbf{M}_v^{IF} \\ \mathbf{0} & \mathbf{M}_v^{FI} & \mathbf{M}_v^{FF} \end{bmatrix};$$

$$\mathbf{B} = \begin{bmatrix} \mathbf{0} & \mathbf{0} & \mathbf{0} \\ \mathbf{0} & \mathbf{K}_v^{II} + \hat{\mathbf{M}}_v^{II} & \mathbf{K}_v^{IF} \\ \mathbf{0} & \mathbf{K}_v^{FI} + \hat{\mathbf{M}}_v^{FI} & \mathbf{K}_v^{FF} \end{bmatrix};$$

$$\mathbf{C} = \begin{bmatrix} \mathbf{K}_u^{SS} & \mathbf{K}_u^{SI} & \mathbf{0} \\ \mathbf{K}_u^{IS} & \mathbf{K}_u^{II} + \hat{\mathbf{K}}_v^{II} & \mathbf{0} \\ \mathbf{0} & \hat{\mathbf{K}}_v^{FI} & \mathbf{0} \end{bmatrix};$$

$$\mathbf{G} = \begin{bmatrix} \mathbf{R}_u^S \\ \mathbf{0} \\ \mathbf{R}_v^F \end{bmatrix} - \begin{bmatrix} \mathbf{F}_u^S \\ \mathbf{F}_u^I + \mathbf{F}_v^I \\ \mathbf{F}_v^F \end{bmatrix}; \quad \mathbf{U} = \begin{bmatrix} \mathbf{u}^S \\ \mathbf{u}^I \\ \mathbf{u}^F \end{bmatrix}$$

In order to solve Eq. (22), the time derivatives need to be discretized. Without loss of generality, after use of the time integration scheme, the coupled discrete finite element Eqs. (22) can be written as

$$\begin{bmatrix} \tilde{\mathbf{K}}_u^{SS} & \tilde{\mathbf{K}}_u^{SI} & \mathbf{0} \\ \tilde{\mathbf{K}}_u^{IS} & \tilde{\mathbf{K}}_u^{II} + \tilde{\mathbf{K}}_v^{II} & \tilde{\mathbf{K}}_v^{IF} \\ \mathbf{0} & \tilde{\mathbf{K}}_v^{FI} & \tilde{\mathbf{K}}_v^{FF} \end{bmatrix} \begin{bmatrix} \mathbf{U}^S \\ \mathbf{U}^I \\ \mathbf{U}^F \end{bmatrix} = \begin{bmatrix} \mathbf{R}_u^S \\ \mathbf{0} \\ \mathbf{R}_v^F \end{bmatrix} - \begin{bmatrix} \tilde{\mathbf{F}}_u^S \\ \tilde{\mathbf{F}}_u^I + \tilde{\mathbf{F}}_v^I \\ \tilde{\mathbf{F}}_v^F \end{bmatrix} \tag{23}$$

where $\tilde{\mathbf{K}}$ represents the linearized coefficient matrix, $\mathbf{U}$ is the vector of incremental nodal point displacements/velocities, $\mathbf{R}$ is the vector of discretized externally applied forces, and the vector $\tilde{\mathbf{F}}$ contains known terms from the linearization and time discretization. Note that $\mathbf{U}^S$ contains displacements, $\mathbf{U}^F$ velocities and in $\mathbf{U}^I$, in general, either velocities or displacements are considered (displacements are preferred since they are the primitive variables).

Equations (23) constitute the fully coupled FSI system to be solved. Either the simultaneous or the partitioned

procedures may be used in the solution, depending on the problem to be analyzed.

It is frequently convenient to discretize an FSI problem using completely different meshes for each field. Usually, due to the nature of fluid flows, finer meshes are needed for the fluid domain (when employing the Navier-Stokes or Euler equations to model the fluid flow) than for the discretization of the structure. However, regardless of the meshes employed in the discretization of the fluid and structure, the equilibrium and compatibility conditions, Eqs. (15) and (16), must be satisfied at the interface.

To guarantee that equilibrium is satisfied, the forces exerted by the fluid onto the structure can be calculated, and this information can be used to construct a part of the fully coupled FSI coefficient matrix that couples with the velocities (the effect of $\tilde{\mathbf{K}}_v^{IF}$ and $\tilde{\mathbf{K}}_v^{II}$ but using velocities as state variables). To compute the components of the mentioned coefficient matrix, first fluid tractions at the interface $\mathbf{f}_F^I(s)$ are calculated, where s represents the interface surface. From the traction values, structural nodal forces exerted by the fluid onto the structure are obtained

$$\mathbf{F} = \int_{S_I} \left(\mathbf{H}^S\right)^T \mathbf{f}_F^I(s)\, ds \tag{24}$$

where $\mathbf{H}^S$ is the structural finite element displacement interpolation matrix evaluated at the interface [Bathe (1996)], T indicates transpose, and S_I refers to the fluid-structure interface. Using a Taylor expansion of the force $\mathbf{F}$ we have,

$$\mathbf{F} = \mathbf{F}_0 + \frac{\partial \mathbf{F}}{\partial \mathbf{v}}\mathbf{v} \tag{25}$$

where $\mathbf{F}_0$ is the "reference" value of $\mathbf{F}$ (obtained from the previous iteration or time/load step), $\mathbf{v}$ the vector of nodal velocity increments and $\partial\mathbf{F}/\partial\mathbf{v}$ can be interpreted as the above mentioned coefficient matrix that couples with nodal fluid velocities.

In addition, compatibility conditions must be satisfied between the fluid and structure at the interface. Since velocities and displacements at the interface are related by the time integration scheme, we can express all the interface degrees of freedom using displacements. Then, using the interpolation functions of the structure, the degrees of freedom corresponding to the fluid can be expressed as a function of the structural displacements. Hence, the fluid displacements (and therefore velocities) are given in terms of the structural displacements thus satisfying the compatibility conditions.

As described above, an FSI finite element model consisting of different types and numbers of elements at the interface, can be considered in a partitioned as well as in a simultaneous solution procedure.

4 Solution Procedures

As mentioned before, two main procedures can be employed in the solution of FSI problems: the simultaneous or direct solution and the partitioned or iterative solution. Each of them will be considered below.

4.1 Partitioned (or Iterative) Solution Procedure

In the partitioned procedure the response of the coupled FSI system is calculated using already developed fluid flow and structural solvers. In this way, modularity is achieved and the complete system is divided into subsystems (which correspond to the fluid and structure/solid, although subdivisions of them can also be considered). This approach allows the solution of large systems.

When employing a partitioned procedure the coefficient matrix of Eq. (23) is expressed as the sum of an implicit and an explicit part. The explicit part is placed on the right-hand side of the equilibrium equations and a predictor (i.e. a known value of the corresponding degrees of freedom) is applied to it. The equations are then solved factorizing only the implicit part of the coefficient matrix. The idea is to partition the coefficient matrix in such a way that the solution of one field is separated from the solution of the other field (with the equations coupled through right-hand side terms). Iterations between the field equations are then necessary, at each time or load step, to guarantee convergence of the FSI solution. Note that in this manner a fully coupled fluid-structure interaction analysis is performed.

In essence, the partitioned procedure can be thought of as a Gauss-Seidel iterative algorithm but the predictor may contain linear combinations of past solutions and their derivatives (see, for example, [Park (1980)], [Park and Felippa (1980)]).

Different schemes can be considered, depending on how the coefficient matrix of Eq. (23) is partitioned and what variables (or combination of variables) are passed between the fields (i.e. the choice of predic-

tors). A general description and applications of partitioned schemes employed in the solution of coupled problems can be found in [Park (1980)], [Park and Felippa (1980)], [Bathe, Zhang and Wang (1995)] [Bathe, Zhang and Ji (1999)] [Piperno, Farhat and Larrouturou (1995)] [Farhat, Lesoinne and Maman (1995)].

One of the most widely employed FSI partitioned schemes (sometimes called the staggered procedure) is described below.

The first step corresponds to the solution of the ALE fluid flow equations using the (already known) displacements and velocities of the interface as boundary conditions. Once the results are obtained, traction vectors exerted by the fluid onto the structure are calculated and applied to the structure as force boundary conditions and the structural equations are solved. The next step is to solve the fluid flow equations again; of course, after having used the calculated structural displacements to update the fluid domain and mesh and the velocities of the interface. The procedure is repeated until convergence of the FSI problem is achieved. In some works the staggered procedure in time is performed without iterations. However, when employing such approach caution is required since the scheme can accumulate significant errors throughout the time integration. For a general FSI problem, therefore, iterations are recommended, although the total cost of the computations can increase significantly.

The main advantage of partitioned procedures is that already developed field codes (for the fluid and structure) can be used, and only the transfer of information between them need to be programmed. The partitioned procedures are most effective in case the coupling between the fluid and the structure is weak, since then the response of each field is not significantly affected. A weak coupling occurs when the structure is very stiff (as compared to the fluid) and hence barely deforms. If a problem with a strong coupling between the fluid and the structure is analyzed using partitioned procedures, either a large amount of iterations is required at each load or time step or a very small time/load step must be employed.

Sometimes, the time resolution of the fluid and structural response is very different and the use of different time steps for the solution of the fluid and the structure is desired. A partitioned procedure can be easily modified to allow such differences in time step, by the use of subcycling [Farhat and Lesoinne (2000)].

In a dynamic problem, it is important to obtain an unconditionally stable numerical scheme in time (for the linearized problem) such that relatively large time steps can be employed in the solution procedure. The stability and accuracy characteristics of different partitioned procedures that involve the solution of FSI problems was studied in [Park, Felippa and DeRuntz (1977)] [Park (1980)] [Park and Felippa (1980)] [Felippa, Park and Farhat (1998)]. Nevertheless, unconditional stability is very difficult to prove and achieve (especially when the Navier-Stokes or Euler equations are used to model the fluid behavior), and partitioned schemes that are *conditionally* stable are employed.

4.2 Simultaneous (or Direct) Solution Procedure

In the simultaneous solution procedure, the equations of motion (23) of the coupled problem are established and solved all together. This procedure is particularly powerful in case the interaction between the fluid and the structure is very strong (i.e. the structural deformation is important). Note that if the structure is very stiff compared to the fluid, a simultaneous solution procedure would not be effective since an ill-conditioned coefficient matrix (for the linearized coupled equations) would result.

Of main concern when employing a simultaneous solution procedure is the number of equations to be solved at the same time. In engineering applications, where large models (consisting of many elements) are employed to accurately characterize the systems under study, computer capacity can become a constraint in the analysis process. In addition, since the finite element discretized equations corresponding to the fluid result in a non-symmetric coefficient matrix (when convective terms are considered), the complete coupled coefficient matrix must be treated as non-symmetric, which increases the amount of computations to obtain the solution. Of course, this increase is not important (relative to the total amount of computations) in case the number of structural degrees of freedom is small compared to the fluid degrees of freedom.

In [Rugonyi and Bathe (2000)] an efficient direct solution procedure was described, which has the advantage that the solution of the structural and fluid equations is not calculated simultaneously. The coupling employed in the scheme is such that the vector $\mathbf{U}^I$ in Eq. (23) contains displacements (and not velocities), since displacements are the primitive variables at the interface and their use

results in a straight-forward coupling of equations. Efficiency in the solution is achieved by employing a substructuring procedure for the solid equations, condensing out the internal structural degrees of freedom prior to the calculation of the solution. In this way, only the degrees of freedom corresponding to the fluid-structure interface are still considered in the solution of the fluid flow variables, but the effect of the structure is fully taken into account at each iteration of the nonlinear problem. Furthermore, using this procedure, advantage is taken of the symmetry of the coefficient matrix corresponding to the solid/structure. Although the condensation procedure increases the bandwidth of the remaining equations, the procedure is effective in case the structural degrees of freedom constitute a large fraction of the total number of degrees of freedom.

4.3 Stability Analysis for the Fluid-Structure Interface

In a dynamic FSI analysis, the selection of appropriate time integration scheme(s), employed to discretize the coupled equations, is important. It is desirable, for many applications, to select an implicit scheme which is unconditionally stable (for the linearized problem), such that the limitations in the time step used are not governed by the numerical stability of the scheme but rather by accuracy considerations (see for example [Bathe (1996)]). Unconditional stability can be achieved for both structural and fluid flow problems by selecting appropriate time integration schemes. However, for the coupled system it may not be easily achieved. A straightforward way of solving the problem seems to be to use the same time integration scheme for both the structure and the fluid, but an inherent difficulty is that the structural equations involve second order derivatives in time, whereas the fluid equations involve only first order derivatives. Transforming the n structural second order differential Eqs. (17) into a system of $2n$ first order differential equations will dramatically increase the cost of the computations. Instead, the equations are best coupled allowing different time integration schemes for the fluid and the structure.

The stability analysis of the coupled FSI problem is complicated since it involves non-symmetric, non-positive-definite matrices that result from the finite element discretization of the Navier-Stokes (or Euler) equations. Nevertheless, first and second order ordinary differential equations in time can be studied to get insight in the numerical stability of the problem.

Consider the following single degree of freedom equations,

$$\begin{aligned} m_s\ddot{x} + k_s x &= r_s \\ m_f\dot{v} + k_f v &= r_f \end{aligned} \tag{26}$$

Assuming that Eqs. (26) represent the structural and fluid equations at the interface, coupling the equations results in,

$$m_s\ddot{x} + m_f\dot{v} + k_f v + k_s x = 0 \tag{27}$$

It is desirable to solve Eq. (27) in such a way that different time integration schemes are used for the variables x and v (although $\dot{x} = v$) but preserving unconditional stability of the numerical discretization.

Let us assume that the variable x is discretized using the trapezoidal rule, that is to say,

$$\begin{aligned} {}^{t+\Delta t}\dot{x} &= \tfrac{2}{\Delta t}\left({}^{t+\Delta t}x - {}^{t}x\right) - {}^{t}\dot{x} \\ {}^{t+\Delta t}\ddot{x} &= \tfrac{4}{\Delta t^2}\left({}^{t+\Delta t}x - {}^{t}x\right) - \tfrac{4}{\Delta t}{}^{t}\dot{x} - {}^{t}\ddot{x} \end{aligned} \tag{28}$$

and that the variable v is descretized using one of the following time integration schemes:

Trapezoidal rule,

$${}^{t+\Delta t}\dot{v} = \frac{2}{\Delta t}\left({}^{t+\Delta t}v - {}^{t}v\right) - {}^{t}\dot{v} \tag{29}$$

Gear's method,

$${}^{t+\Delta t}\dot{v} = \frac{1}{\Delta t}\left(\frac{3}{2}{}^{t+\Delta t}v - 2\,{}^{t}v + \frac{1}{2}{}^{t-\Delta t}v\right) \tag{30}$$

Euler's backward method,

$${}^{t+\Delta t}\dot{v} = \frac{1}{\Delta t}\left({}^{t+\Delta t}v - {}^{t}v\right) \tag{31}$$

Using the compatibility condition, $\dot{x} = v$, and Eqs. (28) and (29), (30) or (31), Eq. (27) can be discretized in time, and the variable to solve for is ${}^{t+\Delta t}x$. The resulting equation can be analyzed for linear stability. Note that using this procedure, ${}^{t+\Delta t}\ddot{x} \neq {}^{t+\Delta t}\dot{v}$. However, this error is acceptable if the equations result in an unconditionally stable scheme.

In [Rugonyi and Bathe (2000)] it was shown that the integration of Eq. (27) is indeed unconditionally stable when Eq. (28) is used to discretize the variable x and either Eq.

(29), (30) or (31) is used to discretize the variable v, and the compatibility condition $\dot{x} = v$ is used.

From the time integration schemes considered, only the Gear method (which is second order accurate in time) and the Euler backward method (which is first order accurate in time) can be recommended in the time discretization of the fluid flow equations since the trapezoidal rule leads to spurious oscillations.

5 Dynamic Stability Analysis of FSI Problems

Consider the following non-dimensional autonomous nonlinear system

$$\dot{\mathbf{x}} = \mathbf{f}(\mathbf{x}) \tag{32}$$

with initial conditions

$$\mathbf{x}(t_0) = \mathbf{x}_0 \tag{33}$$

where $\mathbf{x}$ is a vector containing the system's state variables and $\mathbf{f}$ is a smooth nonlinear function. Let $\mathbf{x}_r(t)$ be the solution of Eqs. (32) and (33), called the reference trajectory.

To assess the dynamic stability of the system of equations with respect to a given reference trajectory, the behavior of small perturbations, $\mathbf{y}(t)$, to the trajectory has to be investigated. Linearizing Eq. (32) about $\mathbf{x}_r(t)$, the equation for the time evolution of perturbations is obtained,

$$\dot{\mathbf{y}} = \left.\frac{\partial \mathbf{f}}{\partial \mathbf{x}}\right|_{\mathbf{x}_r(t)} \mathbf{y} \tag{34}$$

where $\partial\mathbf{f}/\partial\mathbf{x}$ is the Jacobian matrix of the function $\mathbf{f}(\mathbf{x})$.

The system is dynamically stable, with respect to the reference trajectory, if the real parts of the eigenvalues of the Jacobian matrix of $\mathbf{f}(\mathbf{x})$ are negative at all times. On the other hand, if any eigenvalue has a positive real part, the system is unstable, since perturbations grow exponentially fast. In case the maximum real part of the eigenvalues is zero, the stability cannot in general be assessed using a linearized equation of motion (for the perturbations) and the effects of higher order (nonlinear) terms need to be taken into account. It is important to mention that a system can change from being stable to unstable and vice versa as time evolves.

Associated with the long-term stability of a system, the one-dimensional Lyapunov characteristic exponent, LCE, is a measure of the mean asymptotic divergence/convergence of nearby trajectories in *phase space*,

$$\chi(\mathbf{x}_r, \mathbf{y}_0) = \lim_{t\to\infty} \frac{1}{t} \ln \frac{\|\mathbf{y}(t)\|}{\|\mathbf{y}_0\|} \tag{35}$$

where $||\cdot||$ represents a vector norm, and $\mathbf{y}_0$ an initial perturbation vector. The existence of such a limit is given by the Oseledec multiplicative ergodic theorem [Oseledec (1968)]. The LCE is used to investigate whether the asymptotic behavior of a system is chaotic.

A chaotic response is characterized by an aperiodic long-term dynamic behavior that exhibits sensitivity to initial conditions. A consequence is that nearby trajectories in phase space diverge exponentially fast. Therefore the LCE of a chaotic response is positive and the prediction of the system behavior becomes impossible after a certain time t_p [Strogatz (1994)].

[Benettin, Galgani and Strelcyn (1976)] and [Benettin, Galgani, Giorgilli and Strelcyn (1980)] have presented an approach for calculating the LCE of maps and discrete systems of coupled first order differential equations in time. This procedure is used as a basis to develop below a numerical technique to evaluate the LCE of solid and fluid continua discretized using finite element methods.

Considering Eq. (34), and assuming that the Jacobian matrix of $\mathbf{f}(\mathbf{x})$ is not singular at any time, the perturbation at time t can be expressed as,

$$\mathbf{y}(t) = \Phi(t, t_0)\, \mathbf{y}_0 \tag{36}$$

where $\Phi(t, t_0)$ is a mapping matrix from $\mathbf{y}_0$ to $\mathbf{y}(t)$, with the property, for $t_0 < t_1 < t_2$,

$$\mathbf{y}(t_2) = \Phi(t_2, t_1)\, \Phi(t_1, t_0)\, \mathbf{y}_0 \tag{37}$$

If $\mathbf{y}(t)$ is calculated only at certain discrete time steps, t_n ($n = 1, 2, \ldots$), then $\Phi(t_n, t_{n-1})$ can be approximated using Eq. (34) evaluated at $\mathbf{x}_r(t_{n-1})$ and integrated from time t_{n-1} to time t_n. Note that Eq. (32) must also be solved in order to obtain the reference trajectory, $\mathbf{x}_r(t_{n-1})$.

Using a fixed time step Δt, i.e. $t_n = t_0 + n\,\Delta t$, the following quantity can be calculated,

$$k_n = \frac{1}{t_n} \ln \frac{\|\mathbf{y}(t_n)\|}{\|\mathbf{y}_0\|} \tag{38}$$

Comparing Eqs. (35) and (38) it follows that in the limit of $n \to \infty$ and $\Delta t \to 0$, $k_n \to \chi$.

In addition, using Eq. (37) and defining,

$$\begin{aligned} \mathbf{y}_i^* &= \mathbf{\Phi}\left(t_i, t_{i-1}\right) \tilde{\mathbf{y}}_{i-1} \\ d_i &= \| \mathbf{y}_i^* \| \\ \tilde{\mathbf{y}}_i &= \frac{\mathbf{y}_i^*}{d_i} \end{aligned} \tag{39}$$

with an arbitrary initial perturbation satisfying

$$\|\mathbf{y}_0\| = \|\tilde{\mathbf{y}}_0\| = 1 \tag{40}$$

it follows that

$$\left\|\mathbf{y}\left(t_n\right)\right\| = d_n\, d_{n-1} \ldots d_1 \tag{41}$$

Using this result in Eq. (38),

$$k_n = \frac{1}{t_n} \sum_{i=1}^{n} \ln d_i \tag{42}$$

Note that in the numerical calculation of k_n it is important to normalize the perturbations to avoid an overflow of the calculated vector $\mathbf{y}(t)$, in particular when an unstable situation occurs (i.e. $d_i > 1$). In addition, if $\mathbf{x}_0$ lies in the basin of attraction of an attractor (i.e. a fixed point, limit cycle, strange or chaotic attractor), then for $n \rightarrow \infty$, k_n will be independent of the choice of $\mathbf{x}_r$ and $\mathbf{y}_0$, see [Benettin, Galgani and Strelcyn (1976)]. This means that we are restricting the analysis to cases in which a small perturbation to the system does not change completely the nature of the response. In addition, usually, t_0 is chosen as the time for which transient effects of the system response have decayed to save on computation time.

From Eq. (34), $\mathbf{y}(t)$ tends to grow more into the direction of the eigenvector associated with the eigenvalue of largest real part. Nevertheless, components in other directions are also contained in $\mathbf{y}(t)$, especially at the beginning of the computations.

The numerical procedure described for the calculation of the LCE can be extended to the case of a continuum system discretized using finite elements.

Let us first consider the case of a structure/solid medium. The displacements and velocities of the nodal degrees of freedom form the finite element discretized phase space. Therefore, if $\tilde{\mathbf{u}}$ and $\dot{\tilde{\mathbf{u}}}$ correspond to perturbations in the displacements and velocities of the nodal degrees of freedom, and $\mathbf{u}$ and $\dot{\mathbf{u}}$ are the vectors of displacements and velocities of the reference trajectory at time t, the linearized equations for the perturbation can be written as

$$\mathbf{M}_u\, \ddot{\tilde{\mathbf{u}}} + \mathbf{K}_u\left(\mathbf{u}, \dot{\mathbf{u}}\right) \tilde{\mathbf{u}} = \mathbf{0} \tag{43}$$

with initial conditions,

$$\begin{aligned} \tilde{\mathbf{u}}\left(t_0\right) &= \tilde{\mathbf{u}}_0 \\ \dot{\tilde{\mathbf{u}}}\left(t_0\right) &= \dot{\tilde{\mathbf{u}}}_0 \end{aligned} \tag{44}$$

where $\mathbf{M}_u$ and $\mathbf{K}_u$ are the same matrices as in Eq. (17) but it is emphasized here that the tangent stiffness matrix $\mathbf{K}_u$ changes as a function of time with $\mathbf{u}$ and $\dot{\mathbf{u}}$.

Equation (43) could be easily re-written in the form of Eq. (34) with $\mathbf{y}^T = \begin{pmatrix} \tilde{\mathbf{u}} & \dot{\tilde{\mathbf{u}}} \end{pmatrix}$, where the superscript T indicates transpose. However, it is more convenient (from a numerical point of view) to solve directly Eq. (43), using for instance the Newmark method of time integration.

Then, to calculate k_n for each time step, the following procedure is proposed:

- Given the (normalized) "initial" conditions $\tilde{\mathbf{u}}_n$ and $\dot{\tilde{\mathbf{u}}}_n$ at each time step, calculate the accelerations $\ddot{\tilde{\mathbf{u}}}_n$that satisfy Eq. (43).
- Discretize Eq. (43) in time and solve for $\tilde{\mathbf{u}}_{n+1}^*$ and $\dot{\tilde{\mathbf{u}}}_{n+1}^*$.
- Obtain the norm of the perturbation as

$$d_{n+1} = \sqrt{\frac{\left\|\tilde{\mathbf{u}}_{n+1}^*\right\|^2}{L^2} + \frac{\left\|\dot{\tilde{\mathbf{u}}}_{n+1}^*\right\|^2}{V^2}} \tag{45}$$

  where L is a characteristic length of the problem in consideration and $V = \omega_{max}\, L$ is a characteristic velocity, where ω_{max} is the maximum frequency of the finite element model. If instead of choosing the maximum frequency to calculate V, we choose a smaller frequency, numerical problems arise that make k_n grow even when the response is not chaotic. This problem will be discussed in a future paper.

- Normalize the perturbation,

$$\tilde{\mathbf{u}}_{n+1} = \frac{\tilde{\mathbf{u}}_{n+1}^*}{d_{n+1}}; \quad \dot{\tilde{\mathbf{u}}}_{n+1} = \frac{\dot{\tilde{\mathbf{u}}}_{n+1}^*}{d_{n+1}} \tag{46}$$

- Calculate k_{n+1} and advance to the next time step.

An important difference with Eq. (34) is that for a continuum model the perturbations must be compatible with the problem's boundary conditions at all times.

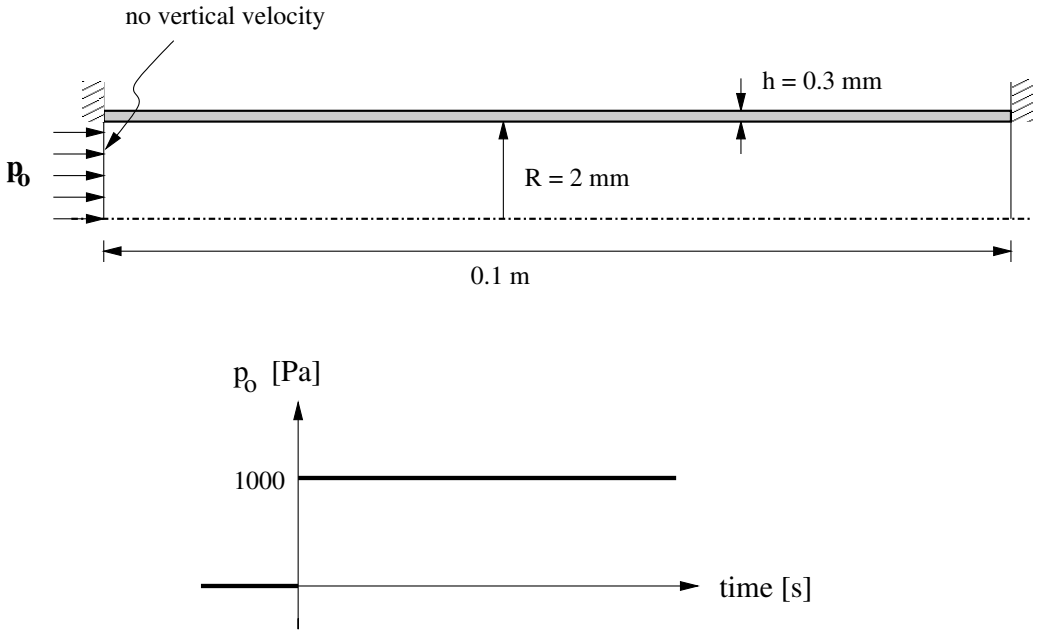

Figure 1 : Geometry and boundary conditions considered for the pressure wave propagation problem.

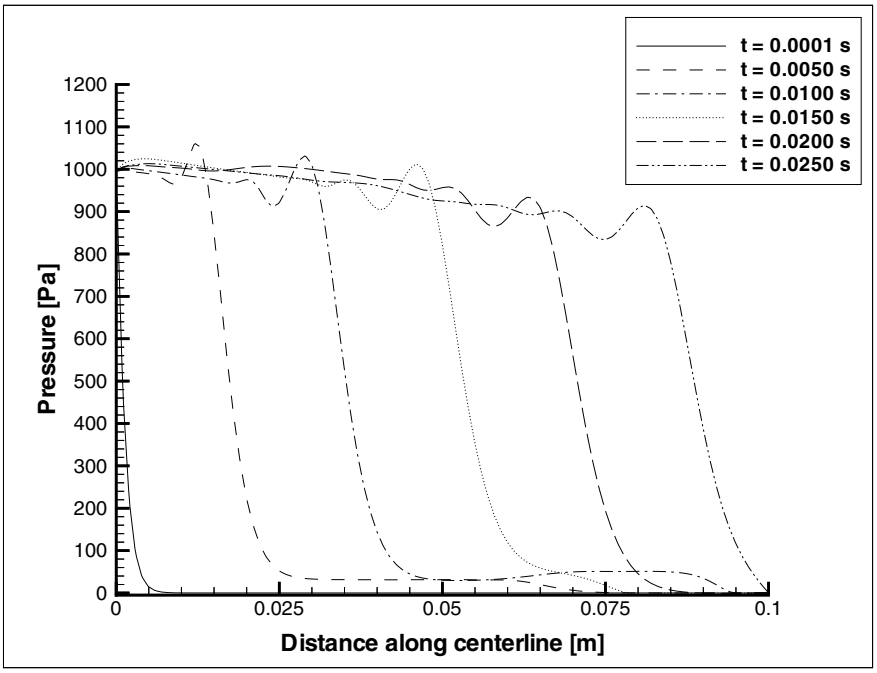

Figure 2 : Pressure propagation inside the tube (the plot shows the value of pressure at the centerline) for different times.

Let us now consider the case of an (almost) incompressible fluid flow in the Eulerian formulation. The (complete) linearized equations for the perturbations are

$$\begin{bmatrix} \mathbf{M}_{vv} & \mathbf{0} \\ \mathbf{0} & \mathbf{M}_{pp} \end{bmatrix} \begin{bmatrix} \dot{\tilde{\mathbf{v}}} \\ \dot{\tilde{\mathbf{p}}} \end{bmatrix} + \begin{bmatrix} \mathbf{K}_{vv} & \mathbf{K}_{vp} \\ \mathbf{K}_{pv} & \mathbf{K}_{pp} \end{bmatrix} \begin{bmatrix} \tilde{\mathbf{v}} \\ \tilde{\mathbf{p}} \end{bmatrix} = \begin{bmatrix} \mathbf{0} \\ \mathbf{0} \end{bmatrix} \tag{47}$$

where $\mathbf{M}$ and $\mathbf{K}$ are the mass and tangent coefficient matrices for the fluid flow. For an incompressible fluid, $\mathbf{M}_{pp}$=$\mathbf{0}$ and $\mathbf{K}_{pp}$=$\mathbf{0}$. Note that in the case of a fluid flow modeled using the Eulerian formulation of motion, the fluid velocities are calculated at certain fixed points in space and therefore instabilities in space (such as turbulence) will affect the value of the calculated k_n and LCE.

Equation (47) can be separated into two equations,

$$\begin{aligned} \mathbf{M}_{vv}\dot{\tilde{\mathbf{v}}} + \mathbf{K}_{vv}\tilde{\mathbf{v}} + \mathbf{K}_{vp}\tilde{\mathbf{p}} &= \mathbf{0} \\ \mathbf{M}_{pp}\dot{\tilde{\mathbf{p}}} + \mathbf{K}_{pv}\tilde{\mathbf{v}} + \mathbf{K}_{pp}\tilde{\mathbf{p}} &= \mathbf{0} \end{aligned} \tag{48}$$

where the first equation corresponds to the perturbation momentum equations and the second one to the continuity condition for the perturbation. It follows that perturbations in velocity and pressure are not completely arbitrary but are constrained by the continuity equation and boundary conditions of the perturbation. For example, considering specifically the case of an incompressible fluid flow, the velocity perturbation must satisfy $\mathbf{K}_{pv}\tilde{\mathbf{v}} = \mathbf{0}$ at all times. The boundary conditions, on the other hand, prevent the pressure perturbation from growing arbitrarily.

The procedure to calculate the successive approximations to the LCE, k_n, is analogous to the one described for the structural equations, taking $\mathbf{y}^T = \begin{pmatrix} \tilde{\mathbf{v}} & \tilde{\mathbf{p}} \end{pmatrix}$, and using an appropriate non-dimensionalization in the calculation of d_i.

When the fluid flow is modeled using the ALE formulation of motion, the situation is more complex. Some of the difficulties are mentioned below.

Since the fluid mesh is moving and the fluid flow velocities are calculated at the mesh nodal points, the obtained velocities do not correspond to fixed points in space nor can they be associated with specific fluid particles. A similar situation occurs with the pressure degrees of freedom. The immediate consequence is that if the mesh points are moving arbitrarily, spurious growth of the perturbations may be included in k_n.

Another difficulty is that in addition to perturbations in velocity and pressure, perturbations in the displacement of certain moving boundaries (such as free surfaces and fluid-structure interfaces) must be considered.

When an FSI problem is solved, the complete linearized equations for the fluid flow coupled with the structure must be considered to evaluate the evolution of perturbations. However, if the main interest lies in the analysis of the behavior of the structural/solid part of the problem, the evolution of the complete vector of perturbations might be calculated but only the displacements and velocities of the structural degrees of freedom used in the calculation of d_i. In this way, while the growth/decay of structural perturbations are considered and specifically followed, the effects of these perturbations in both the structural and fluid domain are taken into account. The difficulties associated with the arbitrary motion of the mesh are then circumvented, since the structural equations are only affected by forces exerted at the interface that are independent of the choice of mesh movement selected. This approach was used in the calculations of the LCE presented below.

It is important to emphasize that as in the case of Eq. (34), the convergence to the LCE can be very slow. However, trends in the behavior of the perturbation norm d_i as a function of time can be used to assess the stability of the system response.

6 Example Problems

In this section we consider the solution of some FSI problems to indicate the current state of analysis capabilities. Further solutions of FSI problems in which the fluid is modeled by the Navier-Stokes equations and full iterations at each time step are performed can be found, for example, in [Moore, Donovan and Powers (1999)] [Tang, Yang, Huang and Ku (1999)] [Wang, Giorges, Park (1999)].

6.1 Pressure Wave Propagation in a Tube

In this first example, a pressure wave propagating inside an axisymmetric tube is considered. A sketch of the problem is shown in Fig. 1. Initially, the tube is filled with a viscous slightly compressible fluid at rest, and at time $t = 0$ a pressure step is applied at the tube inlet (the tube outlet is maintained at zero pressure). As a consequence, a pressure wave develops and starts to travel along and deform the tube as it advances. Figure 2 shows the pressure at the tube centerline for different instants of

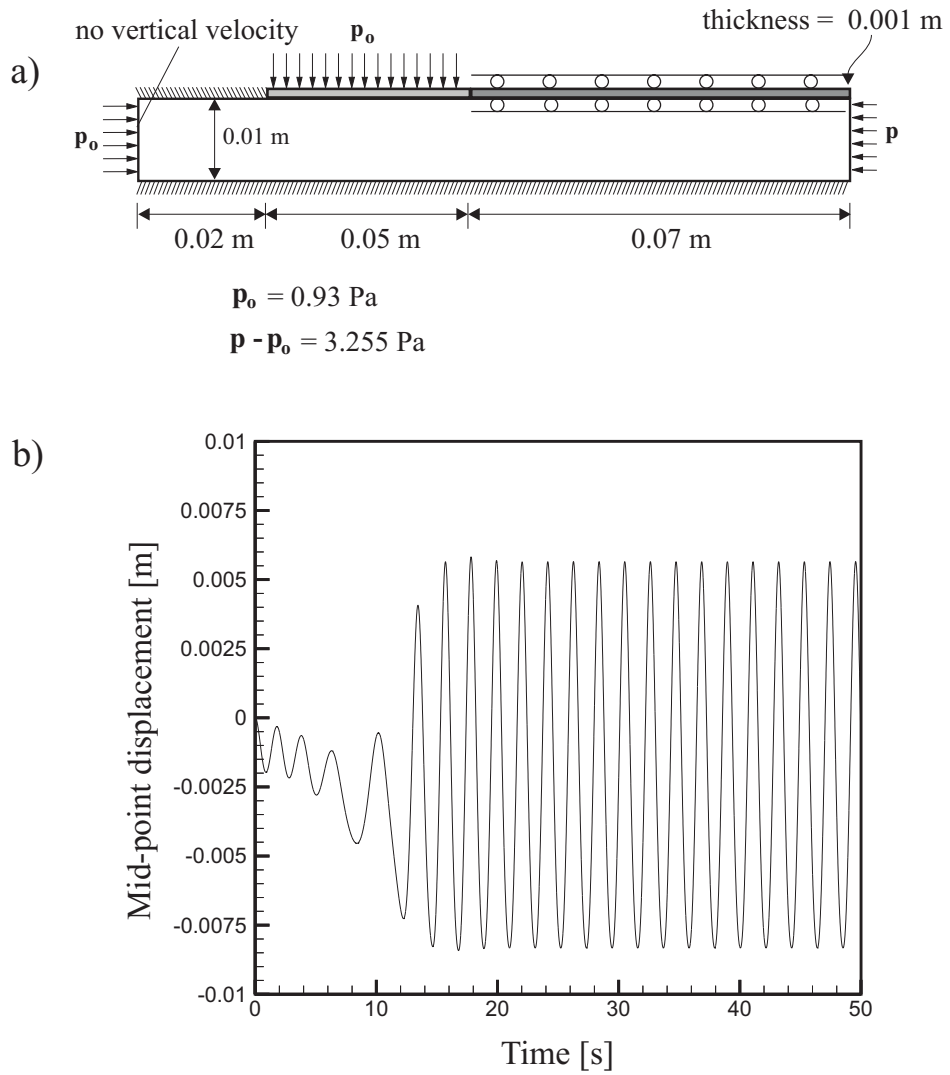

Figure 3 : Collapsible channel problem. a) Geometry and boundary conditions considered, b) Calculated mid-point membrane displacement as a function of time.

time, and it can be observed that the wave moves at an approximately constant propagation speed.

Assuming that the fluid inside the tube is inviscid and incompressible, that the pressure is constant across the tube cross-section and that it is only a function of the value of the transverse area, a simple one-dimensional model of the problem can be obtained [Pedley (1980)]. Under the mentioned assumptions, the pressure wave speed, c, is found to be

$$c = \sqrt{\frac{E\,h}{2\,R\,\rho_F}} \tag{49}$$

where h and R are the undeformed tube thickness and radius respectively, and Eq. (49) is the Moens-Korteweg wave speed equation.

Using Eq. (49) for this problem, a wave speed c = 3.87 m/s is obtained. For the finite element model, the wave speed (see Fig. 2) is approximately c = 3.48 m/s, and therefore about 10% lower. This difference however can be explained by the simplified assumptions in the analytical model.

6.2 Collapsible Channel

The two-dimensional channel shown in Fig. 3 is considered. Part of the upper wall is replaced by a segment

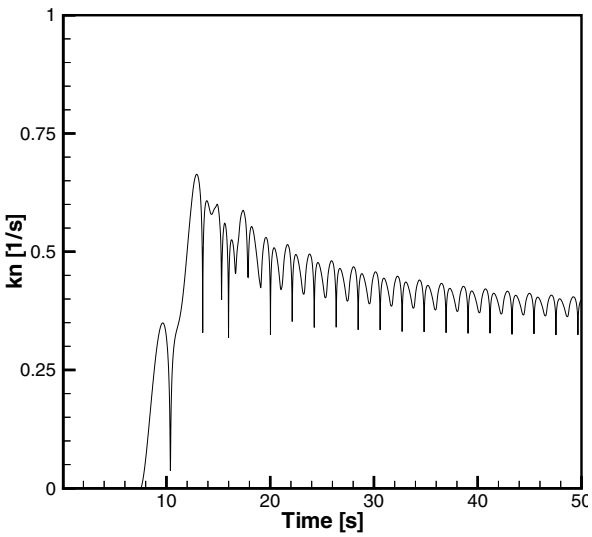

Figure 4 : Successive approximations of the collapsible channel problem LCE as a function of time.

(the collapsible membrane) that can displace both horizontally and vertically and has a pressure applied on it. Another part of the upper wall is replaced by a segment that can only displace horizontally. Initially the channel is filled with a viscous fluid at rest and at time $t = 0$ a pressure difference between inlet and outlet, equal to 3.255 Pa, is applied. The mid-point displacement of the collapsible membrane as a function of time is also shown in Fig. 3, and it can be seen that a limit cycle is developed.

For the case of a limit cycle behavior, the LCE is zero, since all trajectories in the phase space converge to the limit cycle and remain in it. Figure 4 shows the values of k_n (as defined in Eq. (38)) as a function of time. Note that at $t \approx 10$ sec there is a positive jump in the value of k_n corresponding to the growth of the oscillation amplitude leading to a limit cycle behavior (compare with the membrane mid-point displacements of Fig. 3). However, as expected, the amplitude of k_n starts to gradually decrease exponentially afterwards (once the limit cycle response is established). In addition, since only the perturbed displacements of the membrane were taken into account in the calculation of k_n (because ω_{max} is so large that the velocity terms are negligible in the expression of the perturbation norm, Eq. (45)), the value of the system LCE corresponds to the maximum asymptotic value of k_n.

Table 1 : Comparison between calculated and measured temperatures in different locations of the lamp.

Location	Temperature ° F		Difference
	ADNIA	Measured	
DRL Housing	253	245.8	2.9%
DRL Lens	211	206.1	2.4 %
Signal Housing	256	237.4	7.8 %
Signal Lens	156.5	166.1	5.8 %

The calculation of the value of k_n at each time step involves an amount of computations approximately equivalent to an additional iteration step for each time step. Therefore, for this particular example, the calculations require about 20 - 25% of extra computations.

6.3 Fuel Pump

Figure 5 shows the layout of the fuel pump analyzed. A cam rotation moves the bottom diaphragm through a cyclic vertical motion, which pumps fuel to the system. The spring-loaded valves are modeled as structural components, and open and close driven by the pressure differences and fluid flow, see Fig. 6. The amount of mass flow as a function of the cam rotation was of primary interest in this analysis, and Fig. 7 shows a comparison of the results computed with ADINA, obtained by an outside party with the capabilities described in [Bathe, Zhang, and Ji (1999)], and laboratory measured data.

6.4 Analysis of Lamps

The coupled three-dimensional FSI analysis of lamps involves small structural displacements but the complete analysis is highly nonlinear due to the thermal effects and coupling. A typical model of a lamp, shown in Fig. 8, consists of the lens, reflector, bulb and filament, and the fluid (air) assumed to be an incompressible medium. An important part of the analysis is the specular radiation between the components.

Figure 9 gives some computed results and test data and Table 1 lists more comparisons. The computed and experimental results were made available by [Moore, Donovan and Powers (1999)].

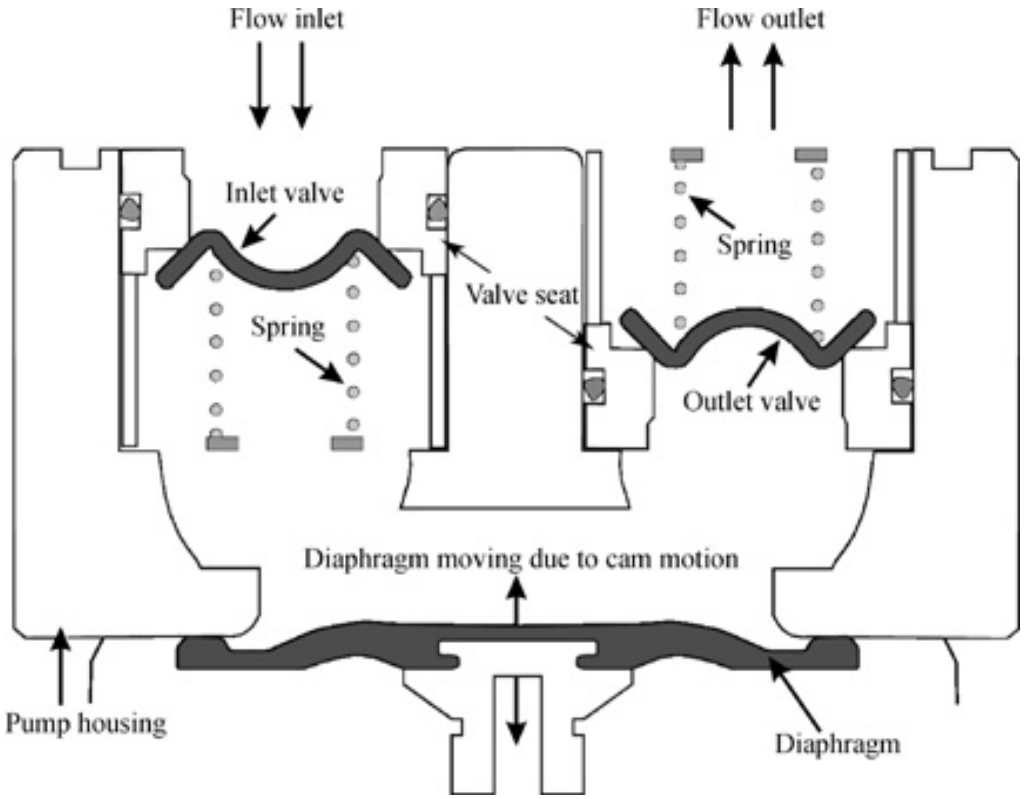

Figure 5 : Fuel pump system considered.

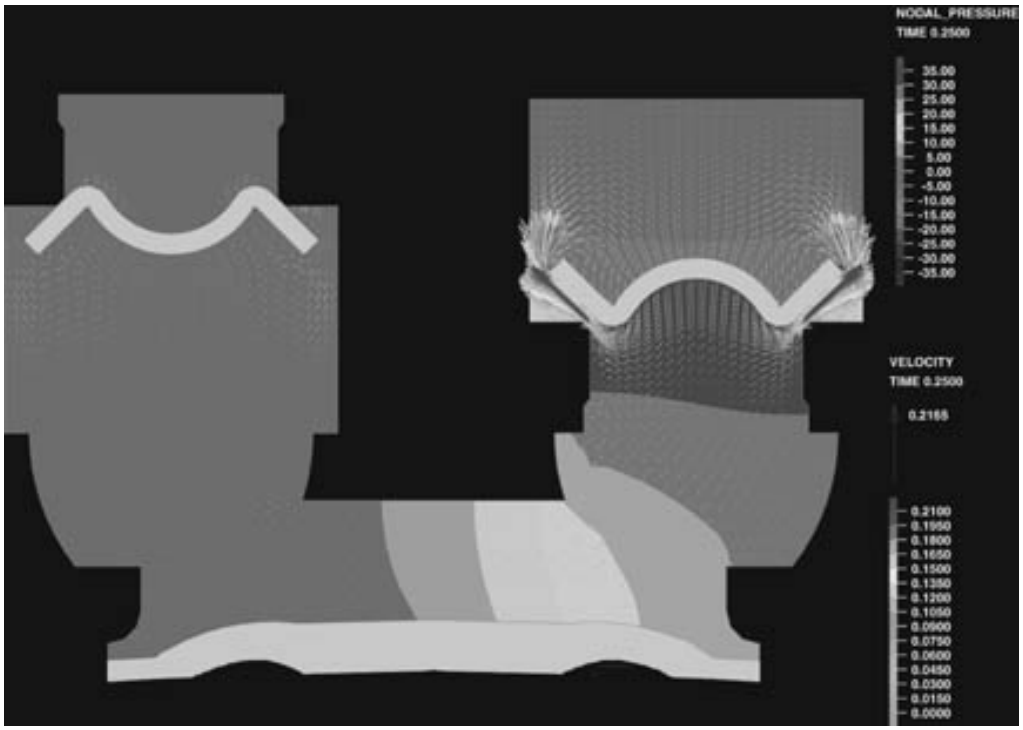

Figure 6 : Pressure difference and velocity field of the fuel inside the pump at a given instant, calculated using ADINA.

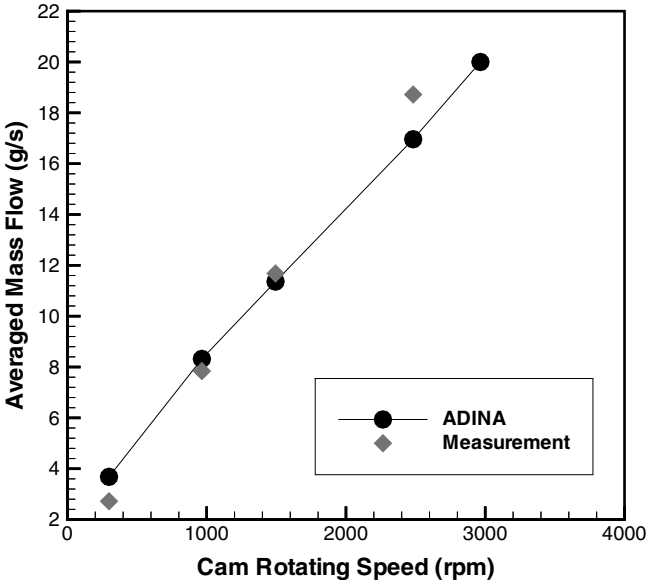

Figure 7 : Comparison of experimental and calculated results for the average mass flow through the pump as a function of the cam rotating speed.

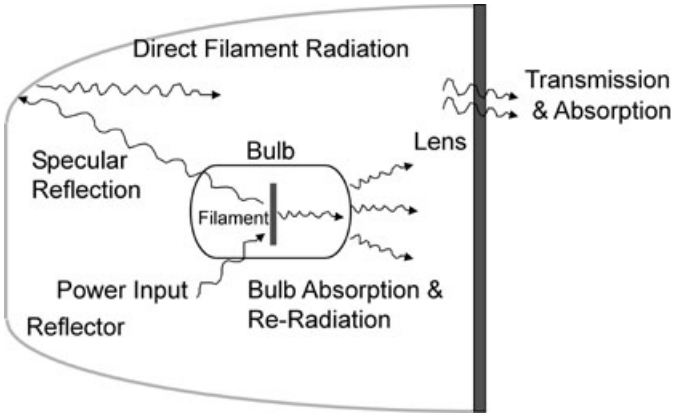

Figure 8 : Lamp model considered.

7 Conclusions

Finite element methods are extensively used in engineering practice to obtain the response of fluid flows and structures, and therefore it is natural to use them to solve FSI problems as well.

Among the solution procedures available for FSI problems, partitioned procedures are very attractive since already developed finite element codes for the fluid flow and structure can be employed. However, still, the exchange of information between the fluid and structural models need to be programmed and the data processing can be costly when different meshes and time steps have to be considered (since information from the discretization of both fields is needed simultaneously). Although powerful, partitioned procedures are not very effective in the solution of FSI problems in which the structure is very flexible and a strong coupling between the fluid and structure results.

Simultaneous procedures, on the other hand, require the coupling and solution of all equations together. The procedures can be enhanced in their effectiveness by using internal condensation of the structural degrees of freedom prior to the solution. These methods are most effective in cases in which there is a strong coupling between the fluid and the structure.

Significant advances have been made in the last few years in the solution of FSI problems, and today very difficult and complex coupled problems can be solved. However, new advances are needed in the characterization of fluid-structure interaction problems. In particular, for certain applications it is important to assess which kind of system response is observed. This can be achieved by calculating the system's response LCE, as presented in this paper. The calculation of the LCE of a continuum system as part of a finite element calculation opens a new and broad range of possibilities in the study and understanding of such systems.

Acknowledgement: We are thankful for the financial support provided to S. Rugonyi by the Rocca Fellowship.

References:

Atluri, S. N. (1984): Alternate stress and conjugate strain measures, and mixed variational formulations involving rigid rotations, for computational analysis of finitely deformed solids, with application to plates and shells: I. Theory. *Computers & Structures*,vol. 18, pp. 93-116.

Bathe, K. J. (1996): *Finite Element Procedures*, Prentice-Hall, New York.

Bathe, K.J.; Zhang, H.; Ji, S. (1999): Finite element analysis of fluid flows fully coupled with structural interactions. *Computers & Structures*, vol. 72, pp. 1-16.

Bathe, K. J.; Zhang H.; Wang M. H. (1995): Finite el-

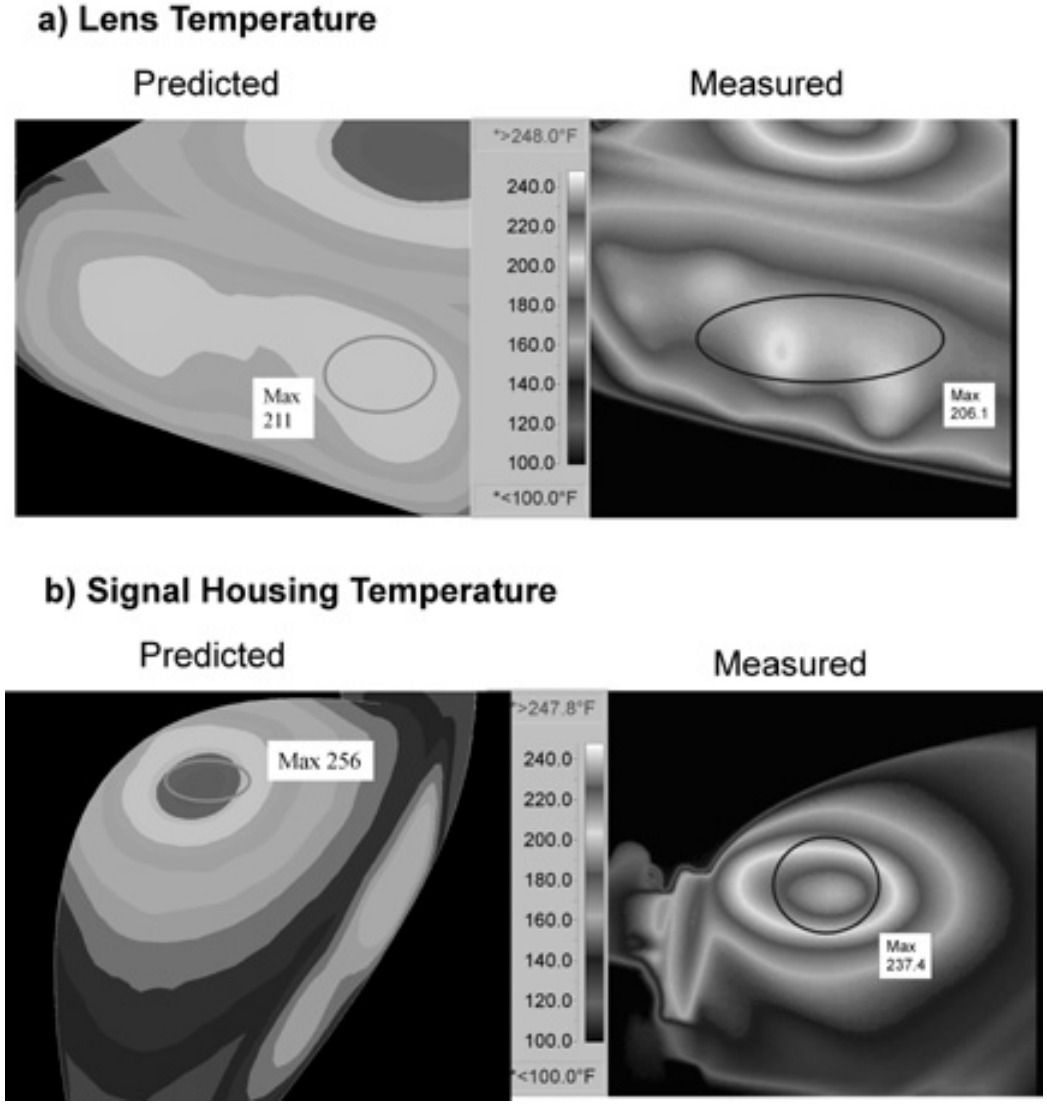

Figure 9 : Comparison between computed and measured temperatures of the lamp lens and signal housing.

ement analysis of incompressible and compressible fluid flows with free surfaces and structural interactions. *Computers & Structures*, vol. 56, pp. 193-213.

Bathe, K. J.; Zhang, H.; Zhang, X. (1997): Some advances in the analysis of fluid flows. *Computers & Structures*, vol. 64, pp. 909-930.

Benettin, G.; Galgani, L.; Giorgilli, A.; Strelcyn, J. M. (1980): Lyapunov characteristic exponents for smooth dynamical systems and for hamiltonian systems; a method for computing all of them. Part 1: Theory. Part 2: Numerical applications. *Meccanica*, vol. 15, pp. 9-30.

Benettin, G.; Galgani, L.; Strelcyn, J. M. (1976): Kolmogorov entropy and numerical experiments. *Physical Review A*, vol. 14, pp. 2338-2345.

Donea, J. (1983): Arbitrary Lagrangian-Eulerian finite element methods. In: T. Belytschko and T.J.R. Hughes (ed) *Numerical Methods for Transient Analysis*, North-Holland, Amsterdam.

Farhat, C.; Lesoinne, M. (2000): Two efficient staggered algorithms for the serial and parallel solution of three-dimensional nonlinear transient aeroelastic problems. *Computer Methods in Applied Mechanics and Engineering*, vol. 182, pp. 499-515.

Farhat, C.; Lesoinne, M.; Maman, N. (1995): Mixed

explicit/implicit time integration of coupled aeroelastic problems: three-field formulation, geometric conservation and distributed solution. *International Journal for Numerical Methods in Fluids*, vol. 21, pp. 807-835.

Felippa, C.A.; Park, K.C.; Farhat C. (1998): Partitioned analysis of coupled systems. In E. Oñate and S. Idelsohn (ed) *Computational Mechanics, Proc. WCCM IV Conf.*, CIMNE, Barcelona.

Moore, W. I.; Donovan, E. S.; Powers, C. R. (1999): Thermal analysis of automative lamps using the ADINA-F coupled specular radiation and natural convection model. *Computers & Structures*, vol. 72, pp. 17-30.

Morand, H. J. P.; Ohayon R. (1995*): Fluid Structure Interaction: Applied Numerical Methods*, John Wiley & Sons.

Olson, L. G.; Bathe, K. J. (1985): Analysis of fluid-structure interactions. A direct symmetric coupled formulation based on a fluid velocity potential. *Computers & Structures*, vol. 21, pp. 21-32.

Oseledec, V. I. (1968): A multiplicative ergodic theorem. Ljapunov characteristic numbers for dynamical systems. *Trans. Moscow Mathematical Society*, vol. 19, pp. 197-231.

Park, K.C. (1980): Partitioned transient analysis procedures for coupled-field problems: stability analysis. *Journal of Applied Mechanics*, vol. 47, pp. 370-376.

Park, K.C.; Felippa, C.A. (1980): Partitioned transient analysis procedures for coupled-field problems: accuracy analysis. *Journal of Applied Mechanics*, vol. 47, pp. 919-926.

Park, K. C.; Felippa, C. A.; DeRuntz, J. A. (1977): Stabilization of staggered solution procedures for fluid-structure interaction analysis. In: T. Belytschko and T.L. Geers (ed) *Computational methods for fluid-structure interaction problems*, ASME Applied mechanics symposia series, AMD - Vol. 26, pp. 95-124.

Pedley, T. J. (1980): *The Fluid Mechanics of Large Blood Vessels*, Cambridge University Press.

Piperno, S.; Farhat, C.; Larrouturou, B. (1995): Partitioned procedures for the transient solution of coupled aeroelastic problems. Part I: Model problem, theory and two-dimensional application. *Computer Methods in Applied Mechanics and Engineering*, vol. 124, pp. 79-112.

Rugonyi, S.; Bathe, K.J. (2000): On the analysis of fully-coupled fluid flows with structural interaction - a coupling and condensation procedure. *International Journal for Computational Civil and Structural Engineering*, vol. 1, pp. 29-41.

Strogatz, S. H. (1994): *Nonlinear Dynamics and Chaos*, Addison-Wesley.

Tang, D.; Yang, C.; Huang, Y.; Ku, D. N. (1999): Wall stress and strain analysis using a three-dimensional thick-wall model with fluid-structure interactions for blood flow in carotid arteries with stenoses. *Computers & Structures*, vol. 72, pp. 341-356.

Wang, X.; Bathe, K.J. (1997): Displacement/pressure based mixed finite element formulations for acoustic fluid-structure interaction problems. *International Journal for Numerical Methods in Engineering*., vol. 40, pp. 2001-2017.

Wang, X.; Giorges, A. G.; Park, C. (1999): Simulation of a deformable ball passing through a step diffuser. *Computers & Structures*, vol. 72, pp. 435-456.